JOURNAL OF MATERIALS SCIENCE **38** (2003) 1013– 1019

Detection of microfracture processes in composite laminates by thermo-acoustic emission

NAK-SAM CHOI
Department of Mechanical Engineering, Hanyang University, 1271, Sa-1dong, Ansan-si, Kyunggi-do 425-791, Korea
E-mail: nschoi@hanyang.ac.kr

YOUNG-BOK KIM, TAE-WON KIM
Department of Mechanical Design, Hanyang University, Sungdong-koo, Seoul, 133-791, Korea

KYONG Y. RHEE
School of Mechanical and Industrial System Engineering, Kyung Hee University, Yongin, 449-701, Korea

The damage process in composite laminates subjected to cryogenic cooling was monitored employing a thermo-acoustic emission (AE) technique. The thermo-AE signals processed with a short-time Fourier transform could be classified into three different types which were correlated with individual microfracture processes. In the initial stage of cryogenic cooling, very strong AE signals with low and high frequency bands were dominantly detected showing that large cracks accompanying fiber breakages were developed mainly. With an increase in the cooling time, weak emissions with low frequency bands became prevalent indicating the propagation of microfractures in the matrix and/or fiber-matrix interface. Similar types of AE signals, however, having weak amplitudes, were also observed for the cryogenically-treated specimens during thermal heating and cooling load cycles. Thus, analysis of thermo-AE behavior through the thermal load cycle led to the nondestructive evaluation for the cryogenic damage of composites.

1. Introduction

Fiber reinforced composite materials have been applied to a variety of components for light-weight structures of aero-space flights, electronic devices and atomic reactors due to their superiority in strength-to-weight and modulus-to-weight. Since composite components are often subjected to external temperature variation when they are used in aerospace environments and in atomic reactors, damages may be induced due to thermal stresses, bringing about a large degradation of the mechanical performance of component structures. Therefore, nondestructive monitoring and evaluation of the damages are significant for the reliability and the safety of composite components.

Because the acoustic emission (AE) measurement technique detects stress waves produced by the transient release of stored strain energy, material fracture state has been evaluated through the analysis of AE data [1–5]. The technique was also applied to the fiber-composites when they were subjected to a thermal load cycle [6, 7]. Many thermo-AEs were observed for the composites containing damages induced by static and dynamic loads, which was thus expected as a nondestructive evaluation technique for damaged composites.

In this paper, the thermo-AE technique is applied to fiber-composite laminates subjected to cryogenic cooling as well as heating and cooling load cycles. Fracture processes being proceeded during cryogenic cooling are monitored through the detection of AE signals according to the fracture types of fibers and matrix. Thermo-AE signals are also detected during heating and cooling load cycles and are classified into different types through a short-time Fourier transform. Those AE data are analyzed for a nondestructive characterization of the cryogenic damages.

2. Experimental

2.1. Composite materials

Composite laminates employed for this study were made of a unidirectional carbon fiber/epoxy prepreg cured in autoclave using a curing cycle recommended by the manufacturer (Hankook Fiber Co.). The curing temperature was 170°C. Rectangular type specimens 30 mm wide, 100 mm long and 3 mm thick were made

by sectioning a manufactured laminate with lay-up angles of $[+90_6/0_6]_s$ using a diamond wheel cutter.

2.2. Acoustic emission measurement during cryogenic cooling

Each specimen was mounted on one end of a wave guide beam by using vacuum silicone grease. An AE transducer (R15, Dunegan Corp.: detectable frequency range 70–600 kHz, resonant frequency 150 kHz) was mounted on the other end of the guide beam. Specimen was rapidly inserted into the cryogenic chamber filled with liquid nitrogen (−191°C) and kept there for 20 minutes.

Just after the insertion of a specimen into the cryogenic chamber, acoustic emission measurement was conducted in real time by an apparatus composed of a cryogenic chamber, a wave guide and the AE measuring system (Mistras-2001, Physical Acoustic Corp.). The generated AE waves in the specimen were detected through the wave guide by the AE transducer. The AE measurement conditions were as follows: Preamplification 40 dB, threshold level 35 dB. From this measurement, the acoustic emission ring-down count rate, hit event counts, amplitude distribution and time-amplitude signals were obtained.

2.3. Acoustic emission measurement during thermal load cycles

After the cryogenic experiment, the specimen and wave guide beam returned to room temperature and then were inserted in an electric furnace. Thermo-acoustic emissions during heating and cooling load cycles were measured by an apparatus consisting of an electric furnace, a wave guide and the AE measuring system. A specimen in the furnace was heated from room temperature to 170°C at a rate of +4.3°C/min and then was naturally cooled in the opened furnace to room temperature. The cooling time was 1.5 hours. The thermal load cycle was repeated three times.

2.4. Ultrasonic C-scan and microscopic fractography

A two-dimensional image of the internal damage distributions in the specimen was observed using a water-immersion type ultrasonic C-scan apparatus. The ultrasonic transducer was of a focusing type, emitting a longitudinal wave of 15 MHz. By placing the ultrasonic focal point at a constant depth beneath the upper surface, the back echo amplitudes were scanned over the full range of the specimen.

From the specimen part which had been confirmed as a cryogenically-damaged region by the ultrasonic C-scan, specimens for optical microscopic observation were extracted using a low-speed diamond wheel cutter (ISOMET, Buehler Co.). After polishing the specimen surface, the microstructure and failures of the specimens were observed using a reflection optical microscope. A specimen part which had been delaminated by cryogenic cooling was sectioned using the low-speed cutter to examine the microfractures appearing on the delamination surface. The part was washed in a distilled water and dried in a vacuum chamber, and then was observed using a scanning electron microscope (SEM).

3. Results and discussion

3.1. Acoustic emission behavior during cryogenic cooling

Fig. 1 shows typical behaviors of AE hit-event rates obtained from a composite specimen for 20 minutes of cryogenic cooling. Histograms in the figure indicate the number of AE hit-events accumulated during each measurement period of 10 seconds. A drastic increase in hit-event rate up to the maximum value around 8000 was exhibited for an initial period of about 2 minutes and then the hit-event rate decreased exponentially. The high activity of AE means that some cracks and/or fractures arose drastically. At the cooling time of 12 minutes, the hit-event rate was as low as about 2000. Such activity of AE in the post stage of cooling may indicate that some local microfractures were still propagative. As understood in thermal stress analysis [7, 8], fractures

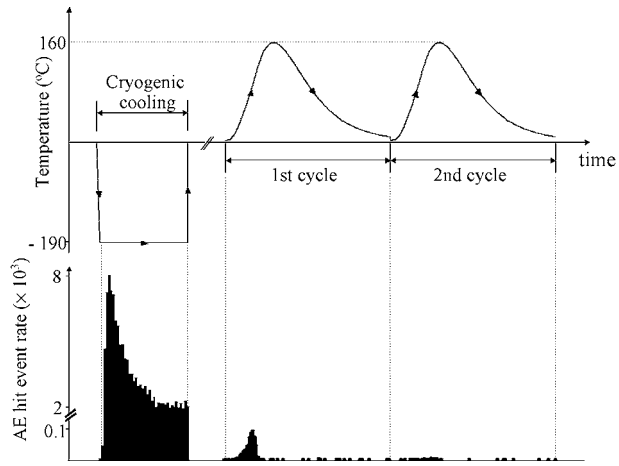

Figure 1 Behaviors of AE hit-event rates from a composite specimen during cryogenic cooling for 20 minutes and, after that, during the 1st and 2nd thermal heating/cooling load cycles.

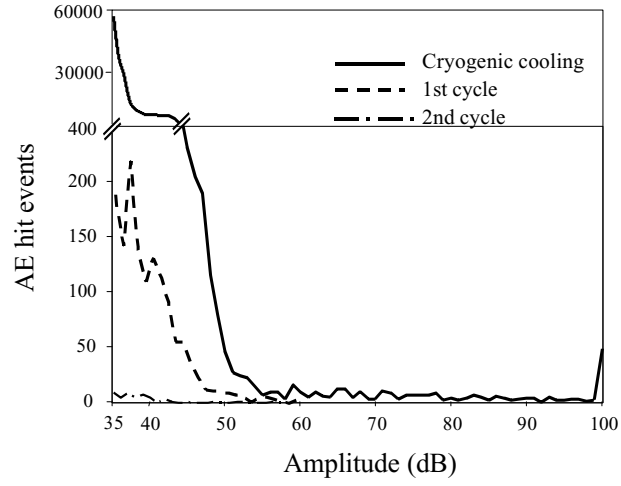

Figure 2 Behaviors of AE hit-events versus peak amplitude distributions of a composite specimen according to various thermal loads in Fig. 1.

could be formed in the free edge region under the influence of thermal in-plane stress and interlaminar stress when the specimen suffered the cryogenic cooling.

Fig. 2 shows diagrams of AE hit-events versus peak amplitude distributions for the specimen in Fig. 1. Although emissions having low amplitudes below 50 dB took the majority beyond 97% of the total events, a minor amount of emissions with large amplitudes 50 to 100 dB were also detected. The strong emissions seem to have been generated during the initiation and propagation of large cracks accompanying the brittle fracture of carbon fibers whose strengths were much bigger than that of the epoxy matrix. On the contrary, the weak emissions might be generated from the local microfracture processes in the matrix and the fiber-matrix interfaces.

3.2. Fracture mechanisms due to cryogenic cooling

A typical ultrasonic C-scan image obtained from a cryogenically-treated composite specimen is exhibited in Fig. 3. The dark image in the figure indicates some fractured and/or delaminated region where the maximum interlaminar stress had been induced by cryogenic cooling as expected in ref. [7, 8]. Fig. 4 is an optical

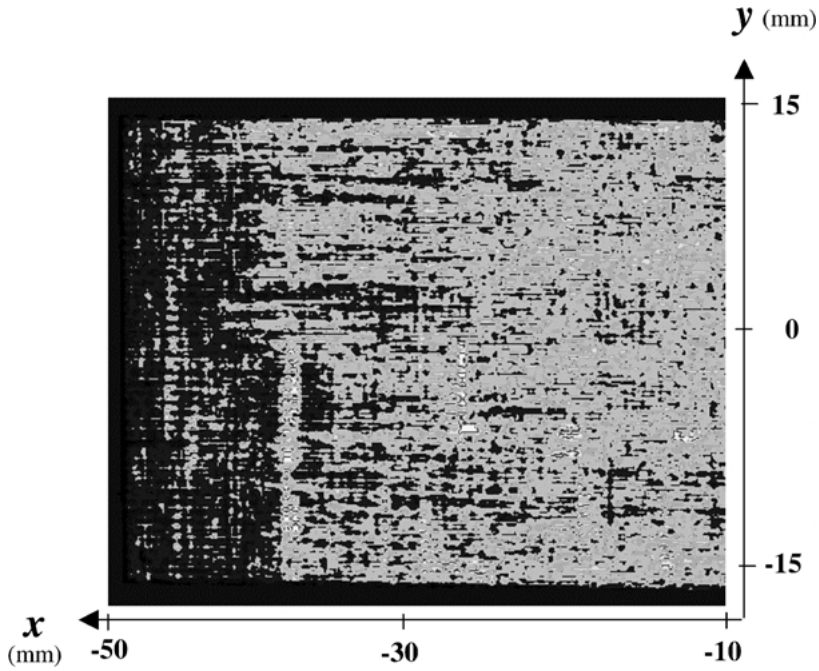

Figure 3 Typical ultrasonic C-scan image of a cryogenically-treated composite specimen: the dark image indicates damaged region due to cryogenic cooling.

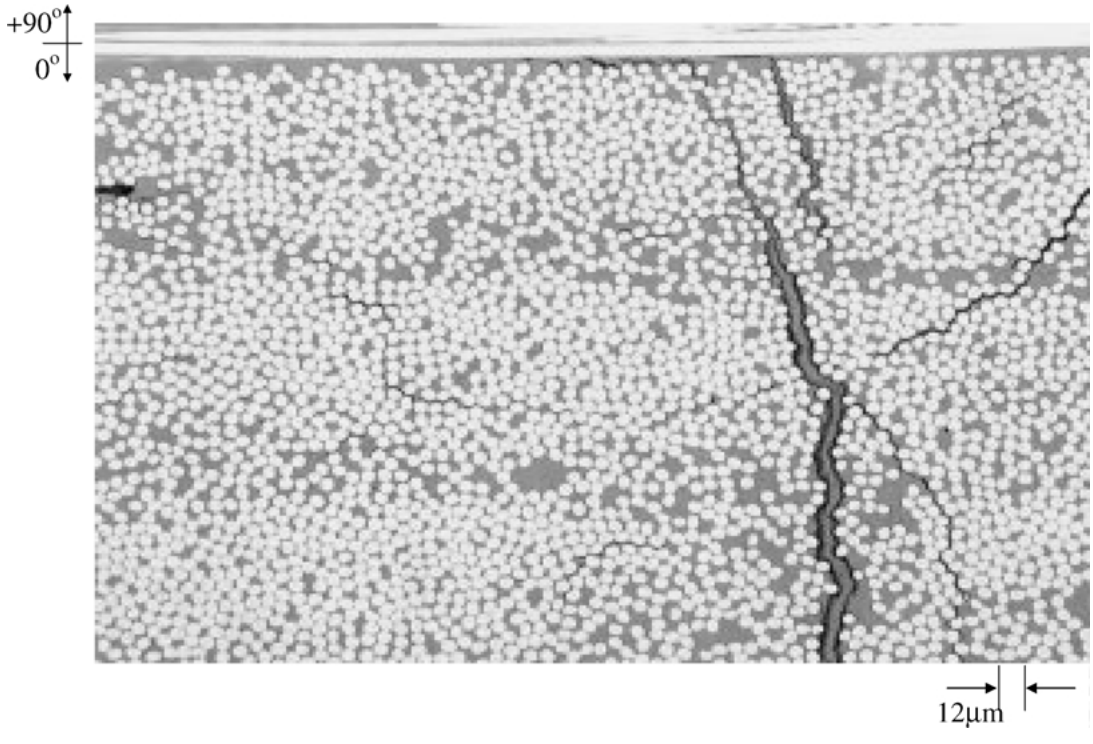

Figure 4 Optical micrograph taken from the cross-section of the damaged free-edge region in Fig. 3.

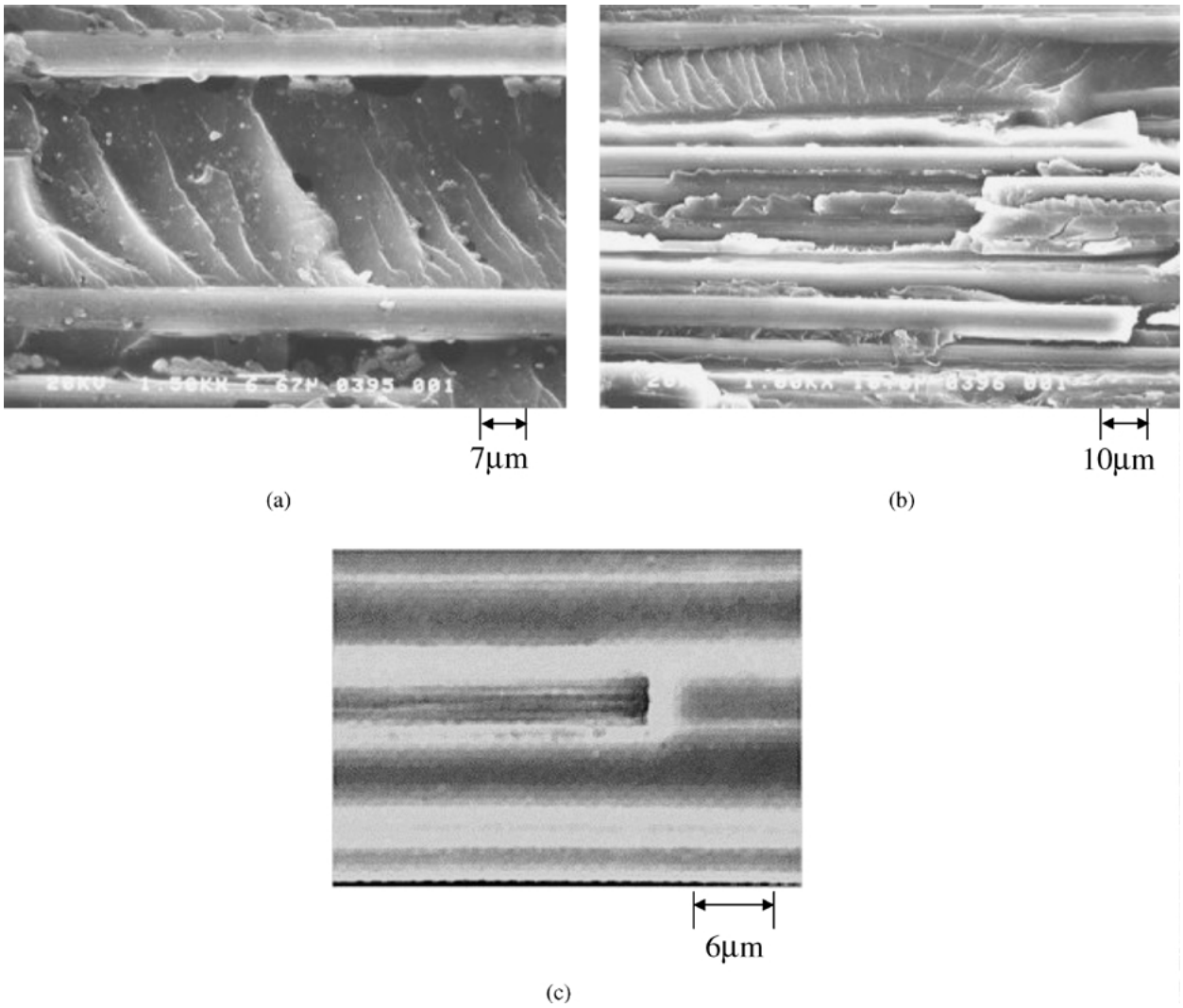

Figure 5 SEM photograph taken from the fracture surface corresponding to the cryogenically damaged portion of a composite specimen: (a) the fracture of matrix and fiber-matrix interface part, (b) the fracture of both fibers and matrix and (c) fiber breakage with little matrix debris.

micrograph taken of the cross-section of the delaminated free edge region in Fig. 3, exhibiting an interlaminar region between the skin (+90°) and the core (0°) layers. The delamination crack near the +90°/0° ply interface propagated into the core layer as a biased local crack, which joined with transverse cracks arisen in the core layer. Those fractures proceeded in a zigzagged way through the matrix resin and around the fiber-matrix interfaces, causing the breakage of some fibers bridged across the crack path.

Fig. 5 shows an SEM photograph taken from the fracture surface corresponding to the delaminated portion of a composite specimen subjected to cryogenic cooling. A type-I fracture observed in Fig. 5a was the typical fracture of the matrix and/or interfaces. This kind of fracture may have generated AE waves with low amplitudes below 50 dB as described in Fig. 2. Fig. 5b exhibits a type-II fracture representing the simultaneous fractures of fibers and matrix. This type of fracture accompanying fiber breakages was liable to generate strong emissions with high amplitudes 50 to 100 dB shown in Fig. 2. Most type-II fractures may have been formed due to the large buildup of interlaminar and in-plane tensile stresses during cryogenic cooling. Fig. 5c shows a type-III fracture, i.e. a fiber breakage with little debris of a matrix fracture. This might also generate strong AE.

3.3. Acoustic emission behavior during thermal load cycles

During a thermal heating and cooling cycle, the cryogenically-treated composite specimen revealed very weak AE activity: the level of AE hit-event rate was only about 1/80 times as large as the maximum event-rate for cryogenic cooling (see Fig. 1). AE amplitudes had a dominant distribution below 45 dB and had the maximum value of 65 dB which was much lower than that for cryogenic cooling (see Fig. 2). Since any differences between ultrasonic C-scan images taken before and after the thermal load cycle were hardly observed, it is thought that during the 1st thermal cycle some abrasive contacts inducing secondary microfractures and thus emitting AE waves arose between upper and lower zig-zagged crack surfaces which had been formed due to cryogenic cooling. The 2nd and 3rd thermal cycles resulted in additional decreases in hit-event rate and lowered the amplitudes below 43 dB. This suggests that frictional and/or abrasive contact forces between zig-zagged crack surfaces became weakened due to

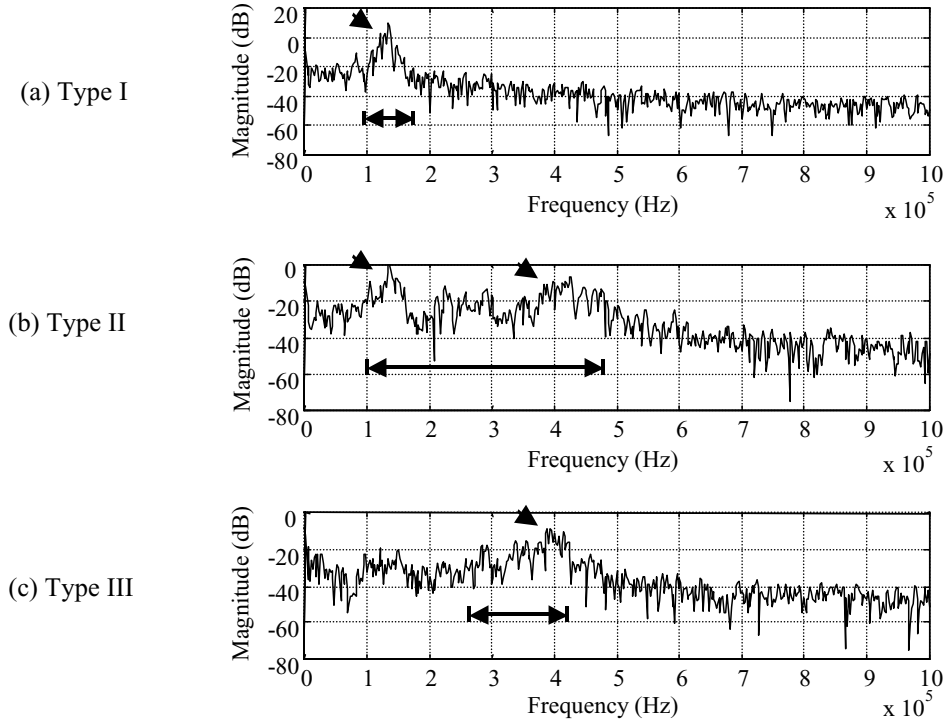

Figure 6 Results of a fast Fourier transform for AE signals obtained during the 1st thermal load cycle: (a) type-I signal with a low frequency band, (b) type-II signal with a combination of low and high frequency bands and (c) type-III signal with a high frequency band.

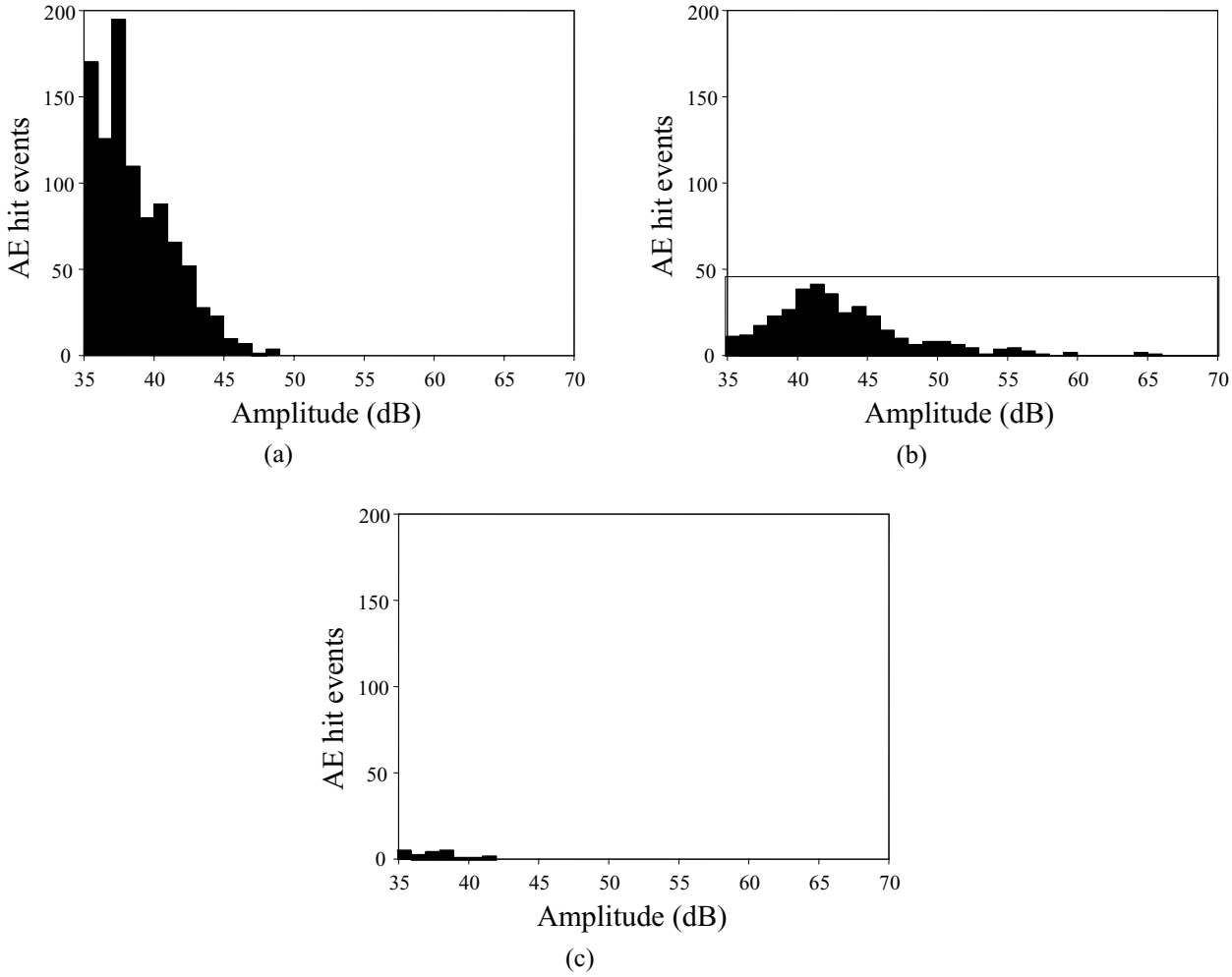

Figure 7 Histograms of AE hit events versus peak amplitude distributions for (a) type-I, (b) type-II and (c) type-III signals in Fig. 6.

relaxation of accumulated residual stresses through the repetitive thermal cycles.

3.4. Nondestructive characterization of microfracture processes by AE signal analysis

The fracture process of fiber composites is accompanied by such microfractures as matrix fractures, fiber-matrix interfacial cracking, fiber breakage and fiber pull-out. Those microfractures may generate AE waves with different frequency bands and different amplitudes according to the individual fracture types and modes [2–5].

A fast Fourier transform (FFT) analysis provided that individual AE signals measured during the 1st thermal cycle could be classified into three different types having different frequency bands. As shown by arrows in Fig. 6a and c, type-I and -III signals had a low frequency band of 70–200 kHz and a dominantly high frequency band of 270–480 kHz, respectively. Type-II signals shown in Fig. 6b had a combination of low and high frequency bands of 70–480 kHz.

Fig. 7 shows histograms of AE hit-events against peak amplitude distribution for each type of AE signal in Fig. 6. Type-I signals had dominant amplitudes below 40 dB and a little distribution up to 47 dB (Fig. 7a). Type-II signals exhibited rather strong amplitudes up to 62 dB and a main distribution of 40–47 dB (see Fig. 7b). This may suggest that type I and II signals were generated from different sources during the thermal cycle. The number of type-II hit-events was relatively small, about 30% of that of type-I hit-events. Type III signals were only 2% of type-I hit-events and their amplitudes were around 37 dB (see Fig. 7c) which was rather similar to the amplitude distribution of type-I signals.

Using a time-frequency analysis method of the short-time Fourier transform (STFT) programmed by the commercial software MATLAB5.3, each AE signal detected from the specimen was processed in a personal computer system. Individual time-frequency signals obtained during the 1st thermal cycle were also classified into three types: Type-I, II and III signals as exhibited in Fig. 8a to c showed frequency bands similar to the FFT results of Fig. 6a to c, respectively. Histograms along the right side of Fig. 8a to c indicate the intensity of time-frequency signals. Amplitudes for each type of signals should have distributions shown in Fig. 7a to c. Considering that the matrix and/or interfacial fracture generates emission of low frequency band [4, 5], it is believed that type-I signals were generated from secondary microfractures in the matrix part contact between upper and lower crack surfaces being moved by thermal deformation mismatch. Because a fiber fracture is liable to produce emissions of high frequency band [4, 5], it is thought that type-III signals were emitted from some abrasive fracturing of fiber ends between crack surfaces. Type-II signals seem to have been generated from fiber fracturing accompanying the matrix microfracture.

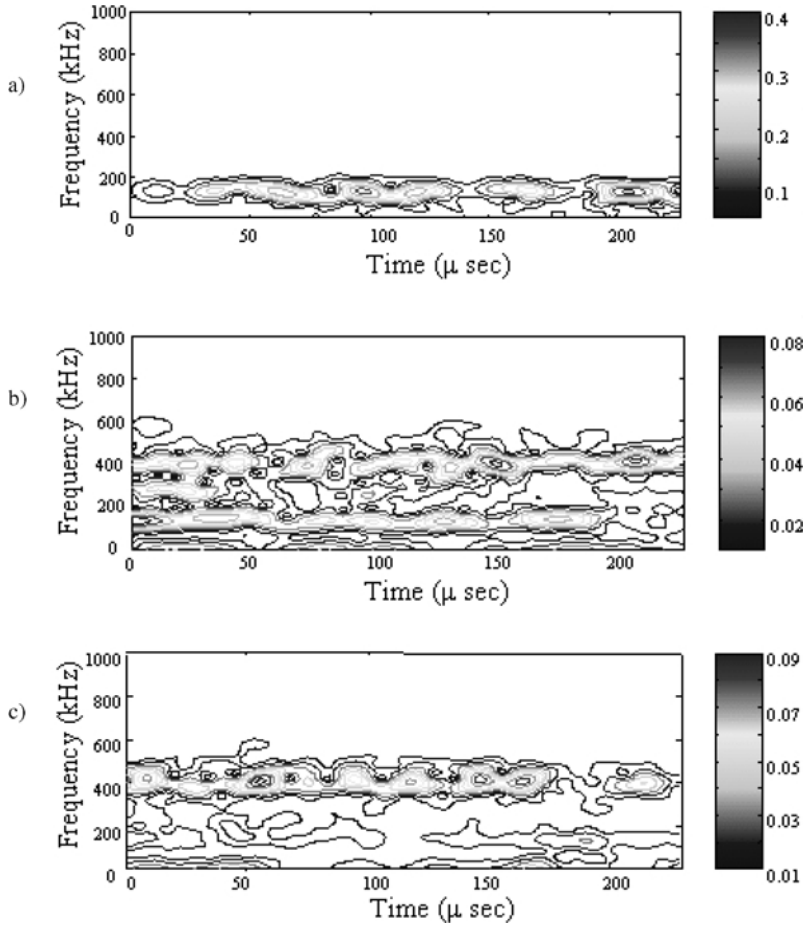

Figure 8 Results of a short-time Fourier transform for AE signals obtained during the 1st thermal load cycle: (a) type-I, (b) type-II and (c) type-III signals.

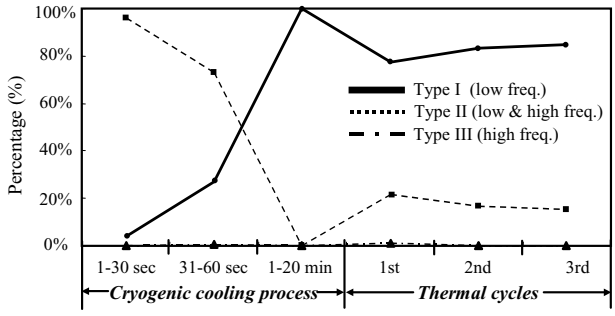

Figure 9 Behaviors of relative percentages in AE hit-events for type-I, type-II and type-III signals detected during the entire process of cryogenic cooling and then the thermal load cycles. Percentage of the signal type may be a nondestructive indicator for the amount of each type of fracture in cryogenically-treated composites.

The three types of AE signals with different frequency bands were detected through the entire thermal process of cryogenic cooling and the thermal load cycles. Relative percentages of those signals obtained during the thermal process are shown in Fig. 9. In the initial stage of 30 seconds after the start of cryogenic cooling, about 97% of detected AE signals was type II showing very high amplitudes of 50 to 100 dB. Type-II signals were still frequent also for the next stage of additional 30 seconds, but their percentage decreased. Type-III signals were infrequent during cryogenic cooling, which suggests that only fiber breakages not accompanying the matrix microfractures were rare. It is believed that large cracks accompanying fiber breakages were dominantly generated in the initial stages.

As the cooling time elapsed, percentage of type-II signals became lessened. However type-I signals with low amplitudes got more and more prevalent, indicating an active propagation of matrix and/or interfacial microfractures. Such behaviors for the three types of AE signals were consistent for different specimens. Therefore, the breakage of bridged-fibers hindering the macroscopic cracking in the initial stage and, after that, the occurrence of numerous microfractures in the matrix and/or the fiber-matrix interface may be the representative damage process of composite laminates during cryogenic cooling.

During the thermal heating and cooling load cycle, amplitudes of AE signals for each type dropped down below one-tenth of the level of amplitudes obtained during cryogenic cooling. Through the repetitive thermal cycles, percentage of type-I signals increased to 86% causing a decrease in that of type-II signals. Because AE sources during the thermal load cycles are considered to be secondary microfractures caused by abrasive and/or frictional contacts between upper and lower zigzagged crack surfaces, percentage of each AE type for a thermal load period may imply a relative degree for the corresponding type of microfractures arisen during cryogenic cooling. Considering that area of fiber breakages was below one-tenth as large as that of matrix and interfacial fractures as shown in Fig. 5, the minor percentage of type II signals obtained during the thermal load cycles may be reasonably understood representing a degree of fiber breakage over the entire crack surface formed in a composite laminate due to cryogenic cooling.

4. Conclusions

Nondestructive characterization of the damage process in composite laminates subjected to cryogenic cooling has been performed employing a thermo-AE technique. Microfracture processes were monitored through the detection of AE waves. The thermo-AE signals processed with a short-time Fourier transform could be classified into three different types which correlated with individual microfracture processes. In the initial stage of cryogenic cooling, very strong AE signals with low and high frequency bands were dominant, which showed the development of large cracks accompanying fiber breakages. As the cooling time passed further, weak emissions with low frequency bands got more prevalent indicating the propagation of microfractures in the matrix and/or fiber-matrix interface. Such fracture processes monitored by thermo-AE measurements might be the representative damage process of composite laminates subjected to cryogenic cooling. Similar types of AE signals, however having weak amplitudes, were obtained also during thermal heating and cooling load cycles after cryogenic cooling. Percentage for each type of AE signals might indicate a relative amount of the corresponding microfracture type. Thus, analysis of thermo-AE behavior through the thermal load cycle offered a nondestructive evaluation of the cryogenic damage of composites.

Acknowledgment

This work was supported by the Brain Korea 21 Project as well as grant No. R01-2000-00294 from the Basic Research Program of the Korea Science & Engineering Foundation.

References

1. J. M. BERTHELOT and J. RHAZI, *Composites Science and Technology* **37** (1990) 411.
2. Standard Practice for Acoustic Emission Examination of Fiberglass Reinforced Plastic Resin (FRP) Tanks/Vessels, ASTM Designation: E1067-01 (American Society for Testing and Materials, West Conshohocken, PA, July 2001).
3. Standard Practice for Acoustic Emission Examination of Reinforced Thermosetting Resin Pipe (RTRP), ASTM Designation: E1118-00 (American Society for Testing and Materials, West Conshohocken, PA, December 2000).
4. N. S. CHOI, K. TAKAHASHI and K.HOSHINO, *NDT & E International* **25** (1992) 271.
5. N. S. CHOI and K. TAKAHASHI, *J. Mater. Sci.* **33** (1998) 2357.
6. N. SATO, T. KURAUCHI and O. KAMIGAITO, *Journal of Composite Materials* **22** (1988) 447.
7. N. S. CHOI and S. H. LEE, *J. Mater. Sci.* **36**(7) (2001) 1685.
8. S. H. LEE, N. S. CHOI and J. K. LEE, *Journal of the Korean Society for Nondestructive Testing* **19** (1999) 347.

Received 19 November 2001
and accepted 16 October 2002